Women with a history of previous childbirths show less evident white matter brain ageing

Irene Voldsbekk*[a,b], Claudia Barth[a], Ivan I. Maximov[a,b,c], Tobias Kaufmann[a,d], Dani Beck[a,b,e], Geneviève Richard[a], Torgeir Moberget[a,b], Lars T. Westlye[a,b,f], Ann-Marie G. de Lange[a,b,g]

[a] *NORMENT, Institute of Clinical Medicine, University of Oslo, & Division of Mental Health and Addiction, Oslo University Hospital, Oslo, Norway*
[b] *Department of Psychology, University of Oslo, Oslo, Norway*
[c] *Department of Health and Functioning, Western Norway University of Applied Sciences, Bergen, Norway*
[d] *Department of Psychiatry and Psychotherapy, University of Tübingen, Germany*
[e] *Sunnaas Rehabilitation Hospital HT, Nesodden, Oslo, Norway*
[f] *KG Jebsen Centre for Neurodevelopmental Disorders, University of Oslo, Oslo, Norway*
[g] *Department of Psychiatry, University of Oxford, Oxford, UK*

Acknowledgements

This research has been conducted using the UK Biobank under Application 27412. The work was performed on the Service for Sensitive Data (TSD) platform, owned by the University of Oslo, operated and developed by the TSD service group at the University of Oslo IT-Department (USIT). Computations were also performed using resources provided by UNINETT Sigma2 – the National Infrastructure for High Performance Computing and Data Storage in Norway. While working on this study, the authors received funding from the Research Council of Norway (I.V; Student scholarship; AM.G.dL.; 286838, T.K.; 276082; L.T.W.; 273345, 249795, 298646, 300768, 223273; C.B.; 250358), the South-East Norway Regional Health Authority (L.T.W.; 2018076, 2019101), and the European Research Council under the European Union's Horizon 2020 research and innovation programme (L.T.W.; 802998).

Data availability statement

The data that support the findings of this study are available through the UK Biobank data access procedures (https://www.ukbiobank.ac.uk/researchers).

*Author correspondence: irene.voldsbekk@psykologi.uio.no

Abstract

Maternal brain adaptations occur in response to pregnancy, but little is known about how parity impacts white matter (WM) microstructure and WM ageing trajectories later in life. Utilising global and regional brain-age prediction based on multi-shell diffusion MRI data, we investigated the association between previous childbirths and WM brain age in 8,895 women in the UK Biobank cohort (age range = 54 - 81 years). The results showed that a higher number of previous childbirths was associated with lower WM brain age, in line with previous studies showing less evident grey matter (GM) brain ageing in parous relative to nulliparous women. Both global WM and GM brain age estimates showed unique contributions to the association with previous childbirths, suggesting partly independent processes. Corpus callosum contributed uniquely to the global WM association with previous childbirths, and showed a stronger relationship relative to several other tracts. While our findings demonstrate a link between reproductive history and brain WM characteristics later in life, longitudinal studies are required to understand how parity influences women's WM trajectories across the lifespan.

Keywords

Brain; aging; pregnancy; parturition; white matter; diffusion tensor imaging

1. Introduction

Maternal brain adaptations have been shown during pregnancy and postpartum, with dynamic alterations across brain regions depending on time since delivery [1, 2, 3, 4, 5]. While some structural brain changes revert post parturition [6], recent studies indicate that some effects of pregnancy may be long-lasting [2, 5], potentially influencing brain trajectories later in life [7, 8, 9, 10]. However, neuroimaging studies of the maternal brain have largely focused on grey matter (GM) volume [1, 2, 10, 11, 12, 13, 4, 14] and cortical thickness [3, 15], and less is known about the effects of pregnancy on brain white matter (WM) microstructure.

Emerging evidence from animal models suggests that pregnancy may induce WM plasticity [16, 17, 18]. Specifically, pregnant mice exhibit increases in oligodendrocyte progenitor cell proliferation, oligodendrocyte generation, and in the number of myelinated axons, indicating an enhanced capacity for myelination in the maternal brain [16]. Pregnancy-induced remyelination may partly explain why pregnancy seem to cause remission of multiple sclerosis (MS), an auto-immune disease that attacks the myelin sheath [19]. In line with this, slower disability progression has been found in parous MS patients after 18 years, compared with nulliparous patients [20]. This effect was strongest in patients that gave birth after disease onset, indicating favourable effects of pregnancy-related adaptations on disease mechanisms in MS.

While the influence of childbirth on WM trajectories in healthy women is largely unknown, one study reported larger regional WM volumes in mothers compared to non-mothers, as well as maternal WM increases that were linked to changes in empathetic abilities during the postpartum period [14]. In line with these findings, a diffusion tensor imaging (DTI) [21] study in rats found that fractional anisotropy (FA), which quantifies the degree of diffusion directionality, in the dentate gyrus increased significantly during pregnancy. However, whole-brain diffusivity also increased in pregnant rats compared to nulliparous rats [17], indicating global changes in the characteristics of molecular water movement - potentially linked to increased extracellular water in the brain during pregnancy [6].

In a recent study comparing longitudinal changes in human brain morphology during pregnancy and two years of pubertal development, no WM changes were observed in mothers, nor in female adolescents [22]. However, as adolescence is known to involve substantial WM remodelling [23, 24, 25, 26, 27], the lack of effects could possibly reflect insensitivity of the method used to assess WM changes (T1-weighted estimation of total WM volume) [22]. In development and ageing studies, WM microstructure is commonly investigated using DTI [21], which yields metrics that are highly

sensitive to age [28]. However, the accuracy of the DTI approach is limited by factors such as, for example, crossing fibres. These obstacles have motivated the development of advanced biophysical diffusion models such as white matter tract integrity (WMTI) [29], which is derived from diffusion kurtosis imaging (DKI) [30], and spherical mean technique (SMT) [31, 32]. Based on assumptions about the underlying microstructure, these models enable estimation of the separable contribution of diffusion in the intra- and extra-axonal space [33], which provides higher biological specificity, i.e. additional information about the microstructural environment [34].

In the current study, we utilised four diffusion models (DTI, DKI, WMTI, SMT) to build predictive models of WM brain ageing, and investigated associations between brain-age estimates and previous childbirths in a sample of 8,895 UK Biobank women (mean age ± standard deviation = 62.45 ± 7.26). In line with studies suggesting that distinct and regional brain-age prediction models may provide additional detail [11, 35, 36, 37], we used separate models to estimate i) global WM ageing, ii) global GM ageing to test for modality-specific contributions, and iii) WM ageing in 12 major WM tracts in order to identify regions of particular importance for maternal brain ageing.

2. Methods and Materials

2.1. Sample characteristics

The initial sample was drawn from the UK Biobank (www.ukbiobank.ac.uk), and included 9,899 women. 899 participants with known brain disorders were excluded based on ICD10 diagnoses (chapter V and VI, field F; *mental and behavioral disorders*, including F00 - F03 for Alzheimer's disease and dementia, and F06.7 *'Mild cognitive disorder'*, and field G; *diseases of the nervous system*, including inflammatory and neurodegenerative diseases (except G55-59; *"Nerve, nerve root and plexus disorders"*). An overview of the diagnoses is provided in the UK Biobank online resources (http://biobank.ndph.ox.ac.uk/showcase/field.cgi?id=41270), and the diagnostic criteria are listed in the ICD10 diagnostic manual (https://www.who.int/classifications/icd/icdonlineversions). In addition, 99 participants were excluded based on magnetic resonance imaging (MRI) outliers (see section 2.2) and 11 participants were excluded based on missing data on the number of previous childbirths, yielding a total of 8,895 participants that were included in the study. Sample demographics are provided in Table 1.

Table 1: Sample demographics. For variables with missing data, sample size (N) is indicated in parentheses. SD = Standard deviation, GCSE = General Certificate of Secondary Education, NVQ = National Vocational Qualification.

Total N	8,895
Age	
Mean ± SD	62.40 ± 7.25
Range [years]	45.13 - 80.66
Number of childbirths (live)	
Mean ± SD	1.74 ± 1.15
Range	0 - 8
N in each group:	
0 = 1,825 — **1** = 1,190 — **2** = 3,911	
3 = 1,535 — **4** = 348 — **5** = 55	
6 = 26 — **7** = 4 — **8** = 1	
Age at first birth (N = 7,066)	
Mean ± SD	26.82 ± 4.99
Range	14 - 47
Years since last birth (N = 5,875)	
Mean ± SD	32.41 ± 9.21
Range	6.77 - 55.19
Menopausal status (N = 8,888)	
Yes	2,745
No	4,767
Not sure, had hysterectomy	925
Not sure, other reason	451
Ethnic background (N = 8,872)	
% White	97.59
% Black	0.54
% Mixed	0.50
% Asian	0.62
% Chinese	0.35
% Other	0.38
% Do not know	0.02
Education (N = 8,868)	
% University/college degree	42.04
% A levels or equivalent	13.97
% O levels/GCSE or equivalent	22.62
% NVQ or equivalent	3.23
% Professional qualification	5.79
% None of the above	6.47
Assessment location (imaging)	
Newcastle	1,419
Cheadle	7,476

2.2. MRI data acquisition and processing

A detailed overview of the UK Biobank data acquisition and protocols is available in [38] and [39]. For the diffusion-weighted MRI data, a conventional Stejskal-Tanner monopolar spin-echo echo-planar imaging sequence was used with multiband factor 3. Diffusion weightings were 1000 and 2000 s/mm^2 and 50 non-coplanar diffusion directions per each diffusion shell. The spatial resolution was 2 mm^3 isotropic, and 5 anterior-posterior vs 3 anterior-posterior images with b = 0 s/mm^2 were acquired. All diffusion data were processed using an optimised diffusion pipeline [40] consisting of 6 steps: noise correction [41, 42], Gibbs-ringing correction [43], estimation of echo-planar imaging distortions, motion, eddy-current and susceptibility-induced distortion corrections [44, 45], spatial smoothing using fslmaths from FSL (version 6.0.1) [46] with a Gaussian kernel of 1mm^3, and diffusion metrics estimation. DTI and DKI derived metrics were estimated using Matlab R2017a (MathWorks, Natick, Massachusetts, USA) as proposed by Veraart and colleagues [47]. The DTI metrics included mean diffusivity, FA, axial diffusivity, and radial diffusivity [21]. The DKI metrics included mean kurtosis, axial kurtosis, and radial kurtosis [30]. WMTI metrics included axonal water fraction, extra-axonal axial diffusivity, and extra-axonal radial diffusivity [29]. SMT metrics included intra-neurite volume fraction, extra-neurite mean diffusivity, and extra-neurite radial diffusivity [31]. See [40] for details on the processing pipeline.

Tract-based spatial statistics (TBSS) was used to extract diffusion metrics in WM [48]. Initially, all maps were aligned to the FMRIB58_FA template supplied by FSL, using non-linear transformation in FNIRT [49]. Next, a mean FA image of 18,600 UK Biobank subjects was obtained and thinned to create a mean FA skeleton. The number N = 18,600 was obtained from the processing of the two first UKB data releases. The maximal FA values for each subject were then projected onto the skeleton to minimise confounding effects due to partial volumes and any residual misalignments. Finally, all diffusion metrics were projected onto the subject-specific skeletons. WM features were extracted based on John Hopkins University (JHU) atlases for white matter tracts and labels (with 0 thresholding) [50], yielding a total of 910 WM features including mean values and regional measures for each of the diffusion model metrics. For the region-specific brain age models, 12 tracts of interest used in previous ageing and development studies were extracted [51, 52]; anterior thalamic radiation (ATR), corticospinal tract (CST) cingulate gyrus (CG), cingulum hippocampus (CING), forceps major (FMAJ), forceps minor (FMIN), inferior fronto-occipital fasciculus (IFOF), inferior longitudinal fasciculus (ILF) superior longitudinal fasciculus (SLF), uncinate fasciculus (UF), superior longitudinal fasciculus temporal (SLFT), and corpus callosum (CC). The diffusion MRI data passed

TBSS post-processing quality control using the YTTRIUM algorithm [53], and were residualised with respect to scanning site using linear models.

For the GM data, raw T1-weighted MRI data for all participants were processed using a harmonised analysis pipeline, including automated surface-based morphometry and subcortical segmentation. In line with recent brain-age studies [10, 36, 54, 55], we utilised a fine-grained cortical parcellation scheme [56] to extract cortical thickness, area, and volume for 180 regions of interest per hemisphere, in addition to the classic set of subcortical and cortical summary statistics from FreeSurfer (version 5.3) [57]. This yielded a total set of 1,118 structural brain imaging features (360/360/360/38 for cortical thickness/area/volume, as well as cerebellar/subcortical and cortical summary statistics, respectively). Linear models were used to residualise the T1-weighted MRI data with respect to scanning site, intracranial volume [58], and data quality using Euler numbers [59] extracted from FreeSurfer. To remove poor-quality data likely due to motion, participants with Euler numbers of standard deviation (SD) $\pm$ 4 were identified and excluded (n = 80). In addition, participants with SD $\pm$ 4 on the global MRI measures mean FA, mean cortical GM volume, and/or subcortical GM volume were excluded (n = 10, n = 5 and n = 4, respectively), yielding a total of 8,895 participants with both WM (diffusion-weighted) and GM (T1-weighted) MRI data.

2.3. Brain-age prediction

Brain-age prediction is a method in which a machine learning algorithm estimates an individual's age based on their brain characteristics [60]. This estimation is then compared to the individual's chronological age to estimate each individual's brain-age gap (BAG), which is used to identify degrees of deviation from normative ageing trajectories. Such deviations have been associated with a range of clinical risk factors [37, 55, 61] as well as neurological and neuropsychiatric diseases [62, 63, 64, 36]. They have also been assessed in previous studies of parity and brain ageing [9, 10, 11, 54].

Separate brain-age prediction models were run for global WM and GM, and for each of the WM tracts using the *XGBoost regressor model*, which is based on a decision-tree ensemble algorithm (`https://xgboost.readthedocs.io/en/latest/python`). XGboost includes advanced regularisation to reduce overfitting [65], and uses a gradient boosting framework where the final model is based on a collection of individual models (`https://github.com/dmlc/xgboost`). For the global WM and GM models, principal component analyses (PCA) were run on the features to reduce computational time. The top 200 PCA components, explaining 97.84% of the total variance, were used as input for the WM model, and the top 700 components, explaining 98.07% of the variance, were

used as input for the GM model. The model parameters were set to *maximum depth* = 4, *number of estimators* = 140, and *learning rate* = 0.1 for the the global and tract-specific WM models, and *maximum depth* = 5, *number of estimators* = 140, and *learning rate* = 0.1 for the global GM model, based on randomised searches with 10 folds and 10 iterations for hyper-parameter optimisation.

The models were run using 10-fold cross-validation, which splits the sample into subsets (folds) and trains the model on all subsets but one, which is used for evaluation. The process is repeated ten times with a different subset reserved for evaluation each time. Predicted age estimates for each participant were derived using the Scikit-learn library (`https://scikit-learn.org`), and BAG values were calculated using (predicted − chronological age). To validate the models, the 10-fold cross validations were repeated ten times, and average R^2, root mean square error (RMSE), and mean absolute error (MAE) were calculated across folds and repetitions.

2.4. Statistical analyses

The statistical analyses were conducted using Python 3.7.6. All variables were standardised (subtracting the mean and dividing by the SD) before entered into the analyses, and p-values were corrected for multiple comparisons using false discovery rate (FDR) correction [66]. Chronological age was included as a covariate in all analyses, adjusting for age-bias in the brain age predictions as well as age-dependence in number of childbirths [67, 68].

2.4.1. Previous childbirths and global WM ageing

To investigate associations between number of previous childbirths and global WM brain ageing, a linear regression analysis was run using *global WM BAG* as the dependent variable, and *number of childbirths* as the independent variable. To control for potential confounding factors, the analysis was rerun including assessment location, education, ethnic background, body mass index (BMI), diabetic status, hypertension, smoking and alcohol intake, menopausal status ('yes', 'no', 'not sure, had hysterectomy', and 'not sure, other reason'), oral contraceptive (OC) and hormonal replacement therapy (HRT) status (previous or current user vs never used), and experience with stillbirth, miscarriage, or pregnancy termination ('yes', 'no') as covariates. In total, 7,725 women had data on all variables and were included in these analyses. In addition, we tested for mean differences in global WM BAG between parous and nulliparous women using an independent samples t-test, and estimated Cohen's d as effect size [69].

2.4.2. Previous childbirths and WM ageing versus GM ageing

To compare the contributions of global WM and GM brain ageing to the association with previous childbirths, a multiple regression analysis was run with both WM and GM based *BAG estimates* as independent variables and *number of childbirths* as the dependent variable, before eliminating one modality at the time to compare the log-likelihood of the full and reduced models. The significance of model differences was calculated using Wilk's theorem [70] as $\sqrt{2(\Delta LL)}$, where $\Delta LL = LL_1 - LL_2$; the difference in log-likelihood between the reduced model (LL_1) and the full model (LL_2).

Next, we tested for differences between the GM and WM BAG associations with number of previous childbirths using a Z test for correlated samples [71] with

$$Z = (\beta_{\mathrm{m1}} - \beta_{\mathrm{m2}}) / \sqrt{\sigma^2_{\mathrm{m1}} + \sigma^2_{\mathrm{m2}} - 2\rho\sigma_{\mathrm{m1}}\sigma_{\mathrm{m2}}}\,, \tag{1}$$

where m1 = model 1 (WM); m2 = model 2 (GM); β = beta coefficients from the linear regressions between number of childbirths and each model; σ = standard errors of the beta coefficients; ρ = age-adjusted correlation between the modality-specific brain age gap estimates.

2.4.3. Previous childbirths and regional WM tracts

To test for unique contributions by each tract to the global WM association with previous childbirths, a multiple regression analysis was run with all tract-specific *BAG estimates* as independent variables and *number of childbirths* as the dependent variable, before eliminating the tracts one at a time to compare the log-likelihood of the full and reduced models. The significance of model differences was calculated using Wilk's theorem as described in Section 2.4.2. In addition, the reduced χ^2 values for each of the models were calculated to account for the difference in number of input variables to the full and reduced models (13 for the full model including 12 tracts + age, versus 11 for the reduced models where each of the tracts were eliminated one by one). Next, we performed separate regression analyses for each tract-specific BAG estimate versus number of childbirths, before testing for differences between the associations using pairwise Z tests for correlated samples (Eq. 1; Section 2.4.2).

3. Results

The age prediction accuracies for the global WM and GM models, as well as each of the the tract-specific WM models are shown in Table 2. The associations between number of previous childbirths and BAG estimates based on each of the predictions are shown in Table 3.

3.1. Previous childbirths and global WM ageing

A higher number of previous childbirths was associated with lower global WM BAG, as shown in Table 3. The model including potential confounding factors showed a corresponding association of $\beta = -0.04$, SE $= 0.007, t = -5.10, p = 3.46 \times 10^{-7}$, indicating that assessment location, education, ethnic background, BMI, diabetic status, hypertension, smoking and alcohol intake, menopausal status, and OC and HRT use could not fully explain the association between number of childbirths and global WM BAG. The mean difference in global WM ageing between parous and nulliparous women was $t = 3.53, p = 4.15 \times 10^{-4}$; effect size $d = 0.09 \pm 0.03$ (d error).

Table 2: Average R^2, root mean square error (RMSE), mean absolute error (MAE), and correlation (r) between predicted and chronological age for the age prediction models. WM = white matter, GM = grey matter; ATR = anterior thalamic radiation; CST = corticospinal tract; CG = cingulate gyrus; CING = cingulum hippocampus; FMAJ = forceps major; FMIN = forceps minor; IFOF = inferior fronto-occipital fasciculus; ILF = inferior longitudinal fasciculus; SLF = superior longitudinal fasciculus; UF = uncinate fasciculus; SLFT = superior longitudinal fasciculus temporal; CC = corpus callosum; CI = confidence interval.

Global predictions					
Modality	R^2	RMSE	MAE	r [95% CI]	p
WM	0.51 ± 0.02	5.06 ± 0.11	4.10 ± 0.09	0.72 [0.71, 0.73]	<0.001
GM	0.32 ± 0.02	5.98 ± 0.13	4.97 ± 0.11	0.57 [0.55, 0.58]	<0.001
Predictions for each WM tract					
Tract	R^2	RMSE	MAE	r [95% CI]	p
ATR	0.31 ± 0.02	6.03 ± 0.13	4.92 ± 0.12	0.56 [0.54, 0.57]	<0.001
CST	0.15 ± 0.02	6.69 ± 0.14	5.53 ± 0.13	0.38 [0.37, 0.40]	<0.001
CG	0.19 ± 0.02	6.54 ± 0.13	5.38 ± 0.12	0.44 [0.42, 0.45]	<0.001
CING	0.12 ± 0.02	6.81 ± 0.14	5.64 ± 0.12	0.34 [0.32, 0.36]	<0.001
FMAJ	0.14 ± 0.02	6.71 ± 0.13	5.55 ± 0.12	0.38 [0.37, 0.41]	<0.001
FMIN	0.26 ± 0.02	6.24 ± 0.13	5.09 ± 0.12	0.51 [0.49, 0.52]	<0.001
IFOF	0.25 ± 0.02	6.29 ± 0.13	5.16 ± 0.12	0.50 [0.48, 0.51]	<0.001
ILF	0.18 ± 0.02	6.55 ± 0.14	5.40 ± 0.13	0.43 [0.41, 0.44]	<0.001
SLF	0.18 ± 0.02	6.54 ± 0.13	5.40 ± 0.12	0.43 [0.41, 0.45]	<0.001
UF	0.18 ± 0.03	6.56 ± 0.13	5.42 ± 0.12	0.42 [0.40, 0.44]	<0.001
SLFT	0.17 ± 0.02	6.58 ± 0.14	5.42 ± 0.13	0.42 [0.41, 0.44]	<0.001
CC	0.25 ± 0.02	6.26 ± 0.13	5.13 ± 0.12	0.50 [0.49, 0.52]	<0.001

Table 3: Associations between each of the brain age gap estimates and number of previous childbirths (β_{CB}, standard error (SE), t, p, and p_{corr}). Chronological age was included in the analyses for covariate purposes and p-values are reported before and after correction for multiple comparisons, with corrected p-values $<$ 0.05 highlighted in bold. WM = white matter, GM = grey matter; ATR = anterior thalamic radiation; CST = corticospinal tract; CG = cingulate gyrus; CING = cingulum hippocampus; FMAJ = forceps major; FMIN = forceps minor; IFOF = inferior fronto-occipital fasciculus; ILF = inferior longitudinal fasciculus; SLF = superior longitudinal fasciculus; UF = uncinate fasciculus; SLFT = superior longitudinal fasciculus temporal; CC = corpus callosum.

Global associations					
Modality	β_{CB}	SE	t	p	p_{corr}
WM	−0.037	0.007	−5.440	5.46×10^{-8}	$\mathbf{2.31 \times 10^{-7}}$
GM	−0.029	0.005	−5.411	6.43×10^{-8}	$\mathbf{2.31 \times 10^{-7}}$
Associations for each WM tract					
Tract	β_{CB}	SE	t	p	p_{corr}
ATR	−0.022	0.006	−3.662	2.51×10^{-4}	$\mathbf{5.03 \times 10^{-4}}$
CST	−0.006	0.004	−1.441	0.149	0.158
CG	−0.013	0.005	−2.734	0.006	**0.010**
CING	−0.013	0.004	−3.167	0.002	**0.003**
FMAJ	−0.009	0.005	−2.023	0.043	0.055
FMIN	−0.021	0.006	−3.734	1.90×10^{-4}	$\mathbf{4.26 \times 10^{-4}}$
IFOF	−0.012	0.006	−2.238	0.025	**0.038**
ILF	−0.008	0.005	−1.586	0.113	0.135
SLF	−0.006	0.005	−1.178	0.239	0.239
UF	−0.007	0.005	−1.462	0.144	0.158
SLFT	−0.011	0.005	−2.150	0.032	**0.044**
CC	−0.029	0.006	−5.245	1.60×10^{-7}	$\mathbf{4.81 \times 10^{-7}}$

3.2. Previous childbirths and WM ageing versus GM ageing

The age prediction based on the WM model showed higher accuracy compared to the GM prediction (R^2 of 0.51 versus 0.32), as shown in Table 3. To directly compare the model predictions, a post-hoc Z test for correlated samples (Eq. 1; Section 2.4.2) was run on the model-specific fits of predicted versus chronological age (Pearson's r values). The result showed a significant difference in model performance in favour of the WM model; Z = -11.90, $p = 1.06 \times 10^{-32}$.

When comparing regression models including both WM and GM-based BAG estimates to models including only one of the modalities, both the WM-based and the GM-based estimates were found to contribute uniquely to the association with number of previous childbirths, as shown in Table 4. The Z test for differences in associations (Eq. 1; Section 2.4.2) revealed similar associations between number of childbirths and WM-based versus GM-based BAG estimates, as shown in Table 5.

Table 4: Difference in log-likelihood (ΔLL) between regression analyses where grey matter (GM) and white matter (WM)-based brain age gap estimates were eliminated one by one, compared to a model where both were included. The log likelihood (LL) value for the model including both modalities was -12471. Reported are p values before and after correction for multiple comparisons, with corrected p-values < 0.05 highlighted in bold.

Left-out modality	LL	ΔLL	Z	p	p_{corr}
WM	-12479	7.750	3.937	3.436e-04	$\mathbf{4.03 \times 10^{-4}}$
GM	-12479	7.592	3.897	4.026e-04	$\mathbf{4.03 \times 10^{-4}}$

Table 5: Difference in the associations (β) between number of previous childbirths and white matter (WM) versus grey matter (GM)-based brain age estimates (Eq. 1). SE = standard error.

$\beta_{WM} \pm$ SE	$\beta_{GM} \pm$ SE	Z	p
-0.037 $\pm$ 0.007	-0.029 $\pm$ 0.005	1.04	0.30

3.3. Previous childbirths and regional WM tracts

Significant ($p < 0.05$) associations between a higher number of previous childbirths and lower WM BAG estimates were found for ATR, CG, CING, FMIN, IFOF, SLFT, and CC, as shown in Table 3. The correlations between the tract-specific BAG estimates are shown in Figure 1. CC contributed uniquely to the global WM association with number of previous childbirths, as shown in Table 6. Pairwise Z tests for differences in associations revealed that ATR and FMIN had significantly stronger associations with previous childbirths compared to SLF, while CC was more strongly associated with previous childbirths than CST, CG, FMAJ, IFOF, ILF, SLF, UF, and SLFT, as shown in Figure 2.

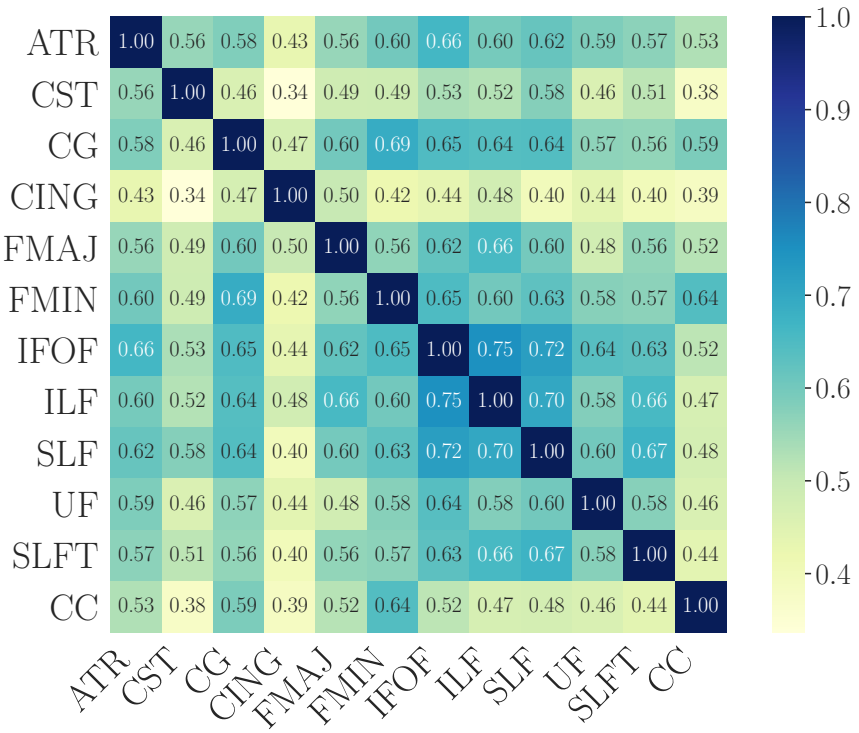

Figure 1: The correlations (Pearson's r) between tract-specific brain age gap (BAG) estimates. The BAG values were first corrected for chronological age using linear models [67], and the residuals were used in the correlation analysis. ATR = anterior thalamic radiation; CST = corticospinal tract; CG = cingulate gyrus; CING = cingulum hippocampus; FMAJ = forceps major; FMIN = forceps minor; IFOF = inferior fronto-occipital fasciculus; ILF = inferior longitudinal fasciculus; SLF = superior longitudinal fasciculus; UF = uncinate fasciculus; SLFT = superior longitudinal fasciculus temporal; CC = corpus callosum.

Table 6: Difference in log-likelihood (ΔLL) between regression analyses against *number of previous childbirths* (including age as a covariate). The difference is calculated between models where all tracts are included and models where single tracts are left out one at a time. Reported are p-values before and after correction for multiple comparisons, with corrected p-values < 0.05 highlighted in bold. X^2_{red} = reduced chi-squared values for each reduced model. For the full model, $X^2_{red} = 0.9686$. ATR = anterior thalamic radiation; CST = corticospinal tract; CG = cingulate gyrus; CING = cingulum hippocampus; FMAJ = forceps major; FMIN = forceps minor; IFOF = inferior fronto-occipital fasciculus; ILF = inferior longitudinal fasciculus; SLF = superior longitudinal fasciculus; UF = uncinate fasciculus; SLFT = superior longitudinal fasciculus temporal; CC = corpus callosum.

Left-out tract	ΔLL	Z	p	p_{corr}	X^2_{red}
ATR	1.855	1.926	0.125	0.645	0.9689
CST	0.082	0.406	0.735	0.783	0.9685
CG	0.024	0.218	0.779	0.783	0.9685
CING	1.599	1.788	0.161	0.645	0.9688
FMAJ	0.389	0.882	0.541	0.783	0.9686
FMIN	0.644	1.135	0.419	0.783	0.9686
IFOF	0.019	0.193	0.783	0.783	0.9685
ILF	0.254	0.712	0.619	0.783	0.9685
SLF	1.077	1.468	0.272	0.683	0.9687
UF	1.030	1.436	0.285	0.683	0.9687
SLFT	0.283	0.752	0.601	0.783	0.9686
CC	5.995	3.463	0.002	**0.024**	0.9698

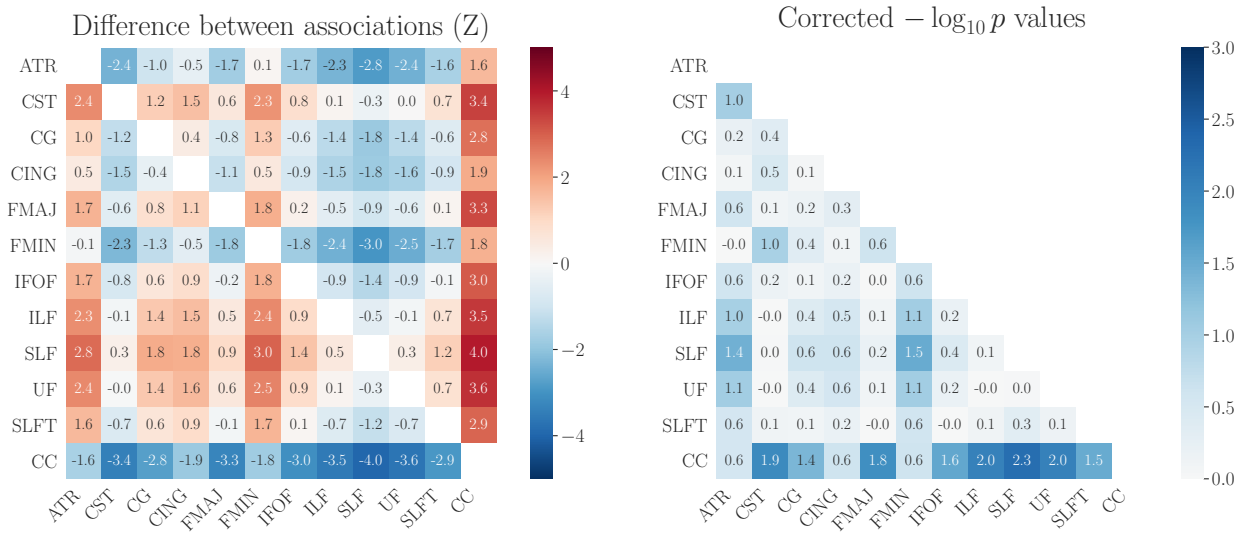

Figure 2: The differences (Z) between tract-specific associations with previous childbirths. The values indicate the association with the tract on the y-axis minus the association with the tract on the x-axis (Eq. 1; Section 2.4.2). The beta values for each association are provided in Table 3 and p values are reported as the common logarithm ($-log_{10}(p)$), corrected for multiple comparisons. A $-log_{10}(p)$ value of > 1.3 corresponds to $p < 0.05$. ATR = anterior thalamic radiation; CST = corticospinal tract; CG = cingulate gyrus; CING = cingulum hippocampus; FMAJ = forceps major; FMIN = forceps minor; IFOF = inferior fronto-occipital fasciculus; ILF = inferior longitudinal fasciculus; SLF = superior longitudinal fasciculus; UF = uncinate fasciculus; SLFT = superior longitudinal fasciculus temporal; CC = corpus callosum.

4. Discussion

The current study investigated the association between previous childbirths and WM brain age by utilising global and region-specific brain-age prediction. The results showed that a higher number of previous childbirths was associated with lower brain age in global WM, as well as in WM tracts including ATR, CG, CING, FMAJ, FMIN, IFOF, SLFT, and CC. CC contributed uniquely to the global WM association with previous childbirths, and showed a stronger relationship with previous childbirths relative to several other tracts. When assessing global WM compared to GM brain age estimates, both modalities showed unique contributions to the association with previous childbirths. Taken together, these results indicate an association between previous childbirths and global WM ageing later in life, with regional effects that may be particularly prominent in CC.

4.1. Previous childbirths and global WM ageing

During pregnancy, several adaptations in the female body and brain take place in order to meet the needs and demands of the offspring, and to secure adequate expression of maternal caregiving [72].

Maternal adaptation in WM may thus be induced to meet these new demands, such as promoting myelination to ensure increased efficiency of neural transmission in relevant WM tracts. While speculative, our results may reflect a long-term benefit of pregnancy-induced WM plasticity, potentially promoting favourable WM trajectories later in life [73]. In support for long-term positive effects of childbirth on WM health, parity is associated with protective effects on age-related decline in learning, memory, and brain health in rats [74]. Further evidence for beneficial effects of parity on brain ageing stems from a study showing that telomeres are significantly elongated in parous relative to nulliparous women [7], suggesting that parity may slow the pace of cellular ageing.

The current results are also in line with previous studies in MS patients showing beneficial effects of pregnancy on WM health [14, 16, 17, 18, 20] and long-term disability progression following childbirth [20]. Oestradiol, a type of oestrogen that increases 300-fold during pregnancy [75], has been linked to pregnancy-induced MS remission [76], likely due to its anti-inflammatory and neuroplastic properties [77]. Postnatally and during the transition to menopause, oestradiol levels drop rapidly and may promote a pro-inflammatory immune environment [78], which has been linked to a high risk of relapse or worsening of symptoms in women suffering from MS [79, 80]. These findings suggest that high oestradiol levels may have protective effects on WM. Further evidence for this stems from hormonal replacement studies in postmenopausal women: long-term oestrogen use has been associated with greater WM volumes [81], indicating a protective effect on WM loss in ageing. However, oestrogen exposure has also been associated with GM atrophy [82] and higher rates of ventricular expansion in menopausal women [83], and some evidence suggests that genetic factors may influence how oestrogen exposure affects brain health [54, 84, 85]. Beside oestrogen, other hormones such as progesterone, prolactin, oxytocin, and cortisol also fluctuate during pregnancy and may regulate WM plasticity [86, 87, 88]. While the influence of hormone exposure on brain ageing trajectories is currently unclear, other pregnancy-induced adaptations such as the proliferation of regulatory T cells or fetal microchimerism may also represent mechanisms underlying potential long-term benefits of pregnancy on brain ageing (for a review see [86]). Future studies may target the links between hormone- and immune-related neuroplasticity in pregnancy, and the potential effect of these processes on women's brain ageing trajectories.

4.2. Modality-specific and regional effects

In line with recent studies demonstrating high age prediction accuracy based on diffusion imaging data [37, 63, 89, 90, 91], the WM prediction showed higher accuracy compared to the GM model,

of which the accuracy corresponded to our previous UK Biobank studies [10, 11, 54]. Importantly, we found unique contributions by both models, suggesting that the diffusion-based WM model may pick up variance not explained by the T1-based GM model. These findings highlight the relevance of assessing brain characteristics using different MRI modalities to increase our understanding of possible long-term effects of pregnancy on the brain.

The most prominent regional WM effect of childbirth was seen in the CC, showing both a unique contribution and a stronger association relative to several other tracts, potentially indicating regional variations. While the volume of most WM tracts increase from childhood to young adulthood, peaks around the fifties, and subsequently declines [28, 51, 92, 93, 94, 52], CC volume has been shown to peak already in the beginning of the thirties, exhibiting an earlier onset of age-related decline relative to other WM tracts [52]. Sex differences have also been found in CC ageing, with steeper volumetric declines in men relative to women [95]. While little is known about pregnancy-induced alterations in specific WM regions, an increased number of myelinated axons in the CC have been found in healthy pregnant rats [16], and increased CC remyelination has been observed in pregnant rat models of demyelination [16, 18]. Although speculative, our findings could potentially reflect a mitigating effect of parity on age-related CC volumetric decline. However, CC is also the most accessible WM structure to investigate, given its size and location in the brain, and the relative simple and coherent microstructural milieu may be easier to resolve using diffusion MRI than other pathways with more complex tissue structure. The tract extraction procedure could thus result in higher signal-to-noise ratio for the CC than for the remaining tracts, rendering it more sensitive to tests of WM associations with childbirth.

4.3. Study limitations

The cross-sectional design of the current study represents a major limitation, and longitudinal studies following women through pregnancy, postpartum, and into midlife and older age are required to infer causality between the observed associations. Furthermore, a complex interplay of numerous underlying processes likely influence the link between parity and WM trajectories. While the current study controls for a range of confounding factors including neurological disease, mental disorders, education, lifestyle behaviours, and cardiovascular risk, the number of children a women gives birth to - as well as their brain health across the lifespan - may also depend on genetic predispositions, life circumstances, and additional aspects of general health.

Our results could potentially reflect long-term effects of pregnancy-related processes such as

myelination. However, the exact neurobiological underpinnings of diffusion metrics cannot be directly inferred, and although we utilised advanced diffusion modelling which is sensitive to biophysical tissue properties [34], the biological substrates underlying these metrics remain to be elucidated by future studies. In addition, controlling for the effect of extracellular water or indices of hydration [96] as well as including measures of WM hyperintensities [97, 98] could potentially provide more accurate models of WM ageing.

While the UK Biobank dataset enables detection of subtle effects due to its large sample size, the cohort is homogeneous with regard to ethnic background (97% white participants in the current study), preventing any conclusion about associations between reproductive history and WM ageing across ethnic groups. The cohort is also characterised by a "healthy volunteer effect" [99], suggesting that it is not representative of the general population [100]. Hence, the presented results may not apply to populations beyond those represented in this cohort. However, in context of the historical lack of research on women's brain health [101], the current results represent a contribution that may prompt further study into how female biology influences neural processes involved in normal ageing - as well as autoimmune conditions and Alzheimer's disease, of which the risks are higher for women relative to men [102, 103].

4.4. Conclusion

In summary, the current study found an association between a higher number of previous childbirths and lower WM brain age, in line with previous studies showing relationships between parity and brain characteristics in midlife and older age [9, 11, 15]. As outlined above, a complex interplay of numerous underlying processes likely influence the link between previous childbirths and brain health in older age. Thus, while our results may suggest that reproductive history influences women's WM ageing trajectories, prospective longitudinal studies assessing this multi-factorial relationship are greatly needed to increase the knowledge about women's brain health across the lifespan.

Author contributions

I.V., L.T.W., and A-M.G.dL. designed the study; I.I.M., T.K., C.B., and A-M.G.dL. processed the data; I.V., D.B., and A-M.G.dL. performed the data analyses; I.V., C.B., I.I.M., T.K., D.B., G.R., T.M., L.T.W., and A-M.G.dL. interpreted the data; I.V. and A-M.G.dL. drafted and finalised the manuscript; C.B., I.I.M., T.K., D.B., G.R., T.M., and L.T.W. critically revised the first draft and approved the final manuscript.

References

[1] P. Kim, J. F. Leckman, L. C. Mayes, R. Feldman, X. Wang, J. E. Swain, The plasticity of human maternal brain: longitudinal changes in brain anatomy during the early postpartum period., Behavioral neuroscience 124 (2010) 695.

[2] E. Hoekzema, E. Barba-Müller, C. Pozzobon, M. Picado, F. Lucco, D. García-García, J. C. Soliva, A. Tobeña, M. Desco, E. A. Crone, et al., Pregnancy leads to long-lasting changes in human brain structure, Nature Neuroscience 20 (2017) 287.

[3] P. Kim, A. J. Dufford, R. C. Tribble, Cortical thickness variation of the maternal brain in the first 6 months postpartum: associations with parental self-efficacy, Brain Structure and Function 223 (2018) 3267–3277.

[4] E. Luders, F. Kurth, M. Gingnell, J. Engman, E.-L. Yong, I. S. Poromaa, C. Gaser, From baby brain to mommy brain: Widespread gray matter gain after giving birth, Cortex (2020).

[5] P. Duarte-Guterman, B. Leuner, L. A. Galea, The long and short term effects of motherhood on the brain, Frontiers in neuroendocrinology (2019).

[6] A. Oatridge, A. Holdcroft, N. Saeed, J. V. Hajnal, B. K. Puri, L. Fusi, G. M. Bydder, Change in brain size during and after pregnancy: study in healthy women and women with preeclampsia, American Journal of Neuroradiology 23 (2002) 19–26.

[7] C. K. Barha, C. W. Hanna, K. G. Salvante, S. L. Wilson, W. P. Robinson, R. M. Altman, P. A. Nepomnaschy, Number of children and telomere length in women: a prospective, longitudinal evaluation, PloS one 11 (2016).

[8] J. L. Pawluski, K. G. Lambert, C. H. Kinsley, Neuroplasticity in the maternal hippocampus: Relation to cognition and effects of repeated stress, Hormones and behavior 77 (2016) 86–97.

[9] K. Ning, L. Zhao, M. Franklin, W. Matloff, I. Batta, N. Arzouni, F. Sun, A. W. Toga, Parity is associated with cognitive function and brain age in both females and males, Scientific reports 10 (2020) 1–9.

[10] A.-M. G. de Lange, T. Kaufmann, D. van der Meer, L. A. Maglanoc, D. Alnæs, T. Moberget, G. Douaud, O. A. Andreassen, L. T. Westlye, Population-based neuroimaging reveals traces of childbirth in the maternal brain, Proceedings of the National Academy of Sciences (2019).

[11] A.-M. G. de Lange, C. Barth, T. Kaufmann, M. Anatürk, S. Suri, K. P. Ebmeier, L. T. Westlye, The maternal brain: Region-specific patterns of brain aging are traceable decades after childbirth, Human Brain Mapping (2020).

[12] N. Lisofsky, J. Wiener, O. de Condappa, J. Gallinat, U. Lindenberger, S. Kühn, Differences in navigation performance and postpartal striatal volume associated with pregnancy in humans, Neurobiology of learning and memory 134 (2016) 400–407.

[13] N. Lisofsky, J. Gallinat, U. Lindenberger, S. Kühn, Postpartal neural plasticity of the maternal brain: Early renormalization of pregnancy-related decreases?, Neurosignals 27 (2019) 12–24.

[14] K. Zhang, M. Wang, J. Zhang, X. Du, Z. Chen, Brain structural plasticity associated with maternal caregiving in mothers: A voxel-and surface-based morphometry study, Neurodegenerative Diseases 19 (2019) 192–203.

[15] E. R. Orchard, P. G. Ward, F. Sforazzini, E. Storey, G. F. Egan, S. D. Jamadar, Cortical changes associated with parenthood are present in late life, bioRxiv (2019) 589283.

[16] C. Gregg, V. Shikar, P. Larsen, G. Mak, A. Chojnacki, V. W. Yong, S. Weiss, White matter plasticity and enhanced remyelination in the maternal cns, Journal of Neuroscience 27 (2007) 1812–1823. doi:10.1523/JNEUROSCI.4441-06.2007.

[17] R. W. Chan, L. C. Ho, I. Y. Zhou, P. P. Gao, K. C. Chan, E. X. Wu, Structural and functional brain remodeling during pregnancy with diffusion tensor mri and resting-state functional mri, PLoS One 10 (2015) e0144328.

[18] S. Kalakh, A. Mouihate, Enhanced remyelination during late pregnancy: involvement of the gabaergic system, Scientific reports 9 (2019) 1–16.

[19] C. Confavreux, M. Hutchinson, M. M. Hours, P. Cortinovis-Tourniaire, T. Moreau, P. in Multiple Sclerosis Group, Rate of pregnancy-related relapse in multiple sclerosis, New England Journal of Medicine 339 (1998) 285–291.

[20] M. B. D'hooghe, G. Nagels, Long-term effects of childbirth in ms, Journal of Neurology, Neurosurgery & Psychiatry 81 (2010) 38–41.

[21] P. J. Basser, J. Mattiello, D. LeBihan, MR diffusion tensor spectroscopy and imaging, Biophysical journal 66 (1994) 259–267.

[22] S. Carmona, M. Martínez-García, M. Paternina-Die, E. Barba-Müller, L. M. Wierenga, Y. Alemán-Gómez, C. Pretus, L. Marcos-Vidal, L. Beumala, R. Cortizo, et al., Pregnancy and adolescence entail similar neuroanatomical adaptations: a comparative analysis of cerebral morphometric changes, Human brain mapping 40 (2019) 2143–2152.

[23] T. Paus, Growth of white matter in the adolescent brain: myelin or axon?, Brain and cognition 72 (2010) 26–35.

[24] N. Barnea-Goraly, V. Menon, M. Eckert, L. Tamm, R. Bammer, A. Karchemskiy, C. C. Dant, A. L. Reiss, White matter development during childhood and adolescence: a cross-sectional diffusion tensor imaging study, Cerebral cortex 15 (2005) 1848–1854.

[25] M. Asato, R. Terwilliger, J. Woo, B. Luna, White matter development in adolescence: a dti study, Cerebral cortex 20 (2010) 2122–2131.

[26] A. Giorgio, K. E. Watkins, G. Douaud, A. James, S. James, N. De Stefano, P. M. Matthews, S. M. Smith, H. Johansen-Berg, Changes in white matter microstructure during adolescence, Neuroimage 39 (2008) 52–61.

[27] A. Giorgio, K. E. Watkins, M. Chadwick, S. James, L. Winmill, G. Douaud, N. De Stefano, P. M. Matthews, S. M. Smith, H. Johansen-Berg, et al., Longitudinal changes in grey and white matter during adolescence, Neuroimage 49 (2010) 94–103.

[28] S. R. Cox, S. J. Ritchie, E. M. Tucker-Drob, D. C. Liewald, S. P. Hagenaars, G. Davies, J. M. Wardlaw, C. R. Gale, M. E. Bastin, I. J. Deary, Ageing and brain white matter structure in 3,513 uk biobank participants, Nature communications 7 (2016) 1–13.

[29] E. Fieremans, J. H. Jensen, J. A. Helpern, White matter characterization with diffusional kurtosis imaging, Neuroimage 58 (2011) 177–188.

[30] J. H. Jensen, J. A. Helpern, A. Ramani, H. Lu, K. Kaczynski, Diffusional kurtosis imaging: the quantification of non-gaussian water diffusion by means of magnetic resonance imaging, Magnetic Resonance in Medicine: An Official Journal of the International Society for Magnetic Resonance in Medicine 53 (2005) 1432–1440.

[31] E. Kaden, N. D. Kelm, R. P. Carson, M. D. Does, D. C. Alexander, Multi-compartment microscopic diffusion imaging, NeuroImage 139 (2016) 346–359.

[32] E. Kaden, F. Kruggel, D. C. Alexander, Quantitative mapping of the per-axon diffusion coefficients in brain white matter, Magnetic resonance in medicine 75 (2016) 1752–1763.

[33] D. S. Novikov, V. G. Kiselev, S. N. Jespersen, On modeling, Magnetic resonance in medicine 79 (2018) 3172–3193.

[34] I. O. Jelescu, M. D. Budde, Design and validation of diffusion mri models of white matter, Frontiers in physics 5 (2017) 61.

[35] H. Eavani, M. Habes, T. D. Satterthwaite, Y. An, M.-K. Hsieh, N. Honnorat, G. Erus, J. Doshi, L. Ferrucci, L. L. Beason-Held, et al., Heterogeneity of structural and functional imaging patterns of advanced brain aging revealed via machine learning methods, Neurobiology of aging 71 (2018) 41–50.

[36] T. Kaufmann, D. van der Meer, N. T. Doan, E. Schwarz, M. J. Lund, I. Agartz, D. Alnæs, D. M. Barch, R. Baur-Streubel, A. Bertolino, et al., Common brain disorders are associated with heritable patterns of apparent aging of the brain, Nature neuroscience 22 (2019) 1617–1623.

[37] S. M. Smith, L. T. Elliott, F. Alfaro-Almagro, P. McCarthy, T. E. Nichols, G. Douaud, K. L. Miller, Brain aging comprises multiple modes of structural and functional change with distinct genetic and biophysical associations, eLife 9 (2020) e52677.

[38] F. Alfaro-Almagro, M. Jenkinson, N. K. Bangerter, J. L. Andersson, L. Griffanti, G. Douaud, S. N. Sotiropoulos, S. Jbabdi, M. Hernandez-Fernandez, E. Vallee, et al., Image processing and quality control for the first 10,000 brain imaging datasets from uk biobank, Neuroimage 166 (2018) 400–424.

[39] K. L. Miller, F. Alfaro-Almagro, N. K. Bangerter, D. L. Thomas, E. Yacoub, J. Xu, A. J. Bartsch, S. Jbabdi, S. N. Sotiropoulos, J. L. Andersson, et al., Multimodal population brain imaging in the uk biobank prospective epidemiological study, Nature neuroscience 19 (2016) 1523.

[40] I. I. Maximov, D. Alnaes, L. T. Westlye, Towards an optimised processing pipeline for diffusion magnetic resonance imaging data: Effects of artefact corrections on diffusion metrics and their age associations in UK biobank, Human Brain Mapping 40 (2019) 4146–4162.

[41] J. Veraart, D. S. Novikov, D. Christiaens, B. Ades-Aron, J. Sijbers, E. Fieremans, Denoising of diffusion MRI using random matrix theory, NeuroImage 142 (2016) 394–406.

[42] J. Veraart, E. Fieremans, D. S. Novikov, Diffusion MRI noise mapping using random matrix theory, Magnetic resonance in medicine 76 (2016) 1582–1593.

[43] E. Kellner, B. Dhital, V. G. Kiselev, M. Reisert, Gibbs-ringing artifact removal based on local subvoxel-shifts, Magnetic resonance in medicine 76 (2016) 1574–1581.

[44] J. L. Andersson, S. N. Sotiropoulos, An integrated approach to correction for off-resonance effects and subject movement in diffusion MR imaging, Neuroimage 125 (2016) 1063–1078.

[45] J. L. Andersson, M. S. Graham, E. Zsoldos, S. N. Sotiropoulos, Incorporating outlier detection and replacement into a non-parametric framework for movement and distortion correction of diffusion MR images, NeuroImage 141 (2016) 556–572.

[46] S. M. Smith, M. Jenkinson, M. W. Woolrich, C. F. Beckmann, T. E. Behrens, H. Johansen-Berg, P. R. Bannister, M. De Luca, I. Drobnjak, D. E. Flitney, et al., Advances in functional and structural MR image analysis and implementation as FSL, Neuroimage 23 (2004) S208–S219.

[47] J. Veraart, J. Sijbers, S. Sunaert, A. Leemans, B. Jeurissen, Weighted linear least squares estimation of diffusion MRI parameters: strengths, limitations, and pitfalls, NeuroImage 81 (2013) 335–346.

[48] S. M. Smith, M. Jenkinson, H. Johansen-Berg, D. Rueckert, T. E. Nichols, C. E. Mackay, K. E. Watkins, O. Ciccarelli, M. Z. Cader, P. M. Matthews, T. E. Behrens, Tract-based spatial statistics: Voxelwise analysis of multi-subject diffusion data, NeuroImage 31 (2006) 1487–1505.

[49] J. L. R. Andersson, M. Jenkinson, S. Smith, Non-linear optimisation, FMRIB Technical Report TR07JA1. FMRIB Analysis Group, Oxford University (2007). URL: http://www.fmrib.ox.ac.uk/analysis/techrep.

[50] S. Mori, S. Wakana, P. C. Van Zijl, L. Nagae-Poetscher, MRI atlas of human white matter, Elsevier, 2005.

[51] S. K. Krogsrud, A. M. Fjell, C. K. Tamnes, H. Grydeland, L. Mork, P. Due-Tønnessen, A. Bjørnerud, C. Sampaio-Baptista, J. Andersson, H. Johansen-Berg, et al., Changes in white matter microstructure in the developing brain—a longitudinal diffusion tensor imaging study of children from 4 to 11 years of age, Neuroimage 124 (2016) 473–486.

[52] L. T. Westlye, K. B. Walhovd, A. M. Dale, A. Bjørnerud, P. Due-Tønnessen, A. Engvig, H. Grydeland, C. K. Tamnes, Y. Østby, A. M. Fjell, Life-span changes of the human brain white matter: diffusion tensor imaging (dti) and volumetry, Cerebral cortex 20 (2010) 2055–2068.

[53] I. I. Maximov, D. van der Meer, A.-M. de Lange, T. Kaufmann, A. Shadrin, O. Frei, T. Wolfers, L. T. Westlye, Fast quality control method for derived diffusion metrics (yttrium) in big data analysis: Uk biobank 18608 example (2020). doi:10.1101/2020.02.17.952697.

[54] A.-M. G. de Lange, C. Barth, T. Kaufmann, I. I. Maximov, D. van der Meer, I. Agartz, L. T. Westlye, Women's brain aging: effects of sex-hormone exposure, pregnancies, and genetic risk for alzheimer's disease, bioRxiv (2020) 826123.

[55] A.-M. G. de Lange, M. Anatürk, T. Kaufmann, J. H. Cole, L. Griffanti, E. Zsoldos, D. Jensen, S. Suri, N. Filippini, A. Singh-Manoux, et al., Multimodal brain-age prediction and cardiovascular risk: The whitehall ii mri sub-study, bioRxiv (2020).

[56] M. F. Glasser, T. S. Coalson, E. C. Robinson, C. D. Hacker, J. Harwell, E. Yacoub, K. Ugurbil, J. Andersson, C. F. Beckmann, M. Jenkinson, et al., A multi-modal parcellation of human cerebral cortex, Nature 536 (2016) 171.

[57] B. Fischl, D. H. Salat, E. Busa, M. Albert, M. Dieterich, C. Haselgrove, A. Van Der Kouwe, R. Killiany, D. Kennedy, S. Klaveness, et al., Whole brain segmentation: automated labeling of neuroanatomical structures in the human brain, Neuron 33 (2002) 341–355.

[58] O. Voevodskaya, A. Simmons, R. Nordenskjöld, J. Kullberg, H. Ahlström, L. Lind, L.-O. Wahlund, E.-M. Larsson, E. Westman, A. D. N. Initiative, et al., The effects of intracranial volume adjustment approaches on multiple regional mri volumes in healthy aging and alzheimer's disease, Frontiers in aging neuroscience 6 (2014) 264.

[59] A. F. Rosen, D. R. Roalf, K. Ruparel, J. Blake, K. Seelaus, L. P. Villa, R. Ciric, P. A. Cook, C. Davatzikos, M. A. Elliott, et al., Quantitative assessment of structural image quality, Neuroimage 169 (2018) 407–418.

[60] J. H. Cole, R. P. Poudel, D. Tsagkrasoulis, M. W. Caan, C. Steves, T. D. Spector, G. Montana, Predicting brain age with deep learning from raw imaging data results in a reliable and heritable biomarker, NeuroImage 163 (2017) 115–124.

[61] J. H. Cole, Multi-modality neuroimaging brain-age in uk biobank: relationship to biomedical, lifestyle and cognitive factors, Neurobiology of Aging (2020).

[62] J. Cole, J. Raffel, T. Friede, A. Eshaghi, W. Brownlee, D. Chard, N. De Stefano, C. Enzinger, L. Pirpamer, M. Filippi, et al., Accelerated brain ageing and disability in multiple sclerosis, bioRxiv (2019) 584888.

[63] J. H. Cole, R. E. Marioni, S. E. Harris, I. J. Deary, Brain age and other bodily 'ages': implications for neuropsychiatry, Molecular psychiatry 24 (2019) 266–281.

[64] K. Franke, C. Gaser, Ten years of brainage as a neuroimaging biomarker of brain aging: What insights have we gained?, Frontiers in Neurology 10 (2019) 789.

[65] T. Chen, C. Guestrin, Xgboost: A scalable tree boosting system, in: Proceedings of the 22nd acm sigkdd international conference on knowledge discovery and data mining, 2016, pp. 785–794.

[66] Y. Benjamini, Y. Hochberg, Controlling the false discovery rate: a practical and powerful approach to multiple testing, Journal of the Royal statistical society: series B (Methodological) 57 (1995) 289–300.

[67] T. T. Le, R. T. Kuplicki, B. A. McKinney, H.-w. Yeh, W. K. Thompson, M. P. Paulus, T. . Investigators, et al., A nonlinear simulation framework supports adjusting for age when analyzing brainage, Frontiers in aging neuroscience 10 (2018).

[68] A.-M. G. de Lange, J. H. Cole, Commentary: Correction procedures in brain-age prediction, NeuroImage: Clinical 26 (2020).

[69] J. Cohen, Statistical power analysis for the behavioral sciences, 2nd edn. á/l, 1988.

[70] S. S. Wilks, The large-sample distribution of the likelihood ratio for testing composite hypotheses, The annals of mathematical statistics 9 (1938) 60–62.

[71] D. W. Zimmerman, Correcting two-sample" z" and" t" tests for correlation: An alternative to one-sample tests on difference scores., Psicologica: International Journal of Methodology and Experimental Psychology 33 (2012) 391–418.

[72] C. K. Barha, L. A. Galea, The maternal'baby brain'revisited, Nature neuroscience 20 (2017) 134.

[73] R. A. Hill, A. M. Li, J. Grutzendler, Lifelong cortical myelin plasticity and age-related degeneration in the live mammalian brain, Nature neuroscience 21 (2018) 683–695.

[74] J. D. Gatewood, M. D. Morgan, M. Eaton, I. M. McNamara, L. F. Stevens, A. H. Macbeth, E. A. Meyer, L. M. Lomas, F. J. Kozub, K. G. Lambert, et al., Motherhood mitigates aging-related decrements in learning and memory and positively affects brain aging in the rat, Brain research bulletin 66 (2005) 91–98.

[75] H. Schock, A. Zeleniuch-Jacquotte, E. Lundin, K. Grankvist, H.-Å. Lakso, A. Idahl, M. Lehtinen, H.-M. Surcel, R. T. Fortner, Hormone concentrations throughout uncomplicated pregnancies: a longitudinal study, BMC pregnancy and childbirth 16 (2016) 146.

[76] R. Voskuhl, Hormone-based therapies in ms., International MS journal 10 (2003) 60–66.

[77] C. K. Barha, L. A. Galea, Influence of different estrogens on neuroplasticity and cognition in the hippocampus, Biochimica et Biophysica Acta (BBA)-General Subjects 1800 (2010) 1056–1067.

[78] J. Pfeilschifter, R. Köditz, M. Pfohl, H. Schatz, Changes in proinflammatory cytokine activity after menopause, Endocrine reviews 23 (2002) 90–119.

[79] A. Langer-Gould, S. M. Huang, R. Gupta, A. D. Leimpeter, E. Greenwood, K. B. Albers, S. K. Van Den Eeden, L. M. Nelson, Exclusive breastfeeding and the risk of postpartum relapses in women with multiple sclerosis, Archives of neurology 66 (2009) 958–963.

[80] M. Tutuncu, J. Tang, N. A. Zeid, N. Kale, D. J. Crusan, E. J. Atkinson, A. Siva, S. J. Pittock, I. Pirko, B. M. Keegan, et al., Onset of progressive phase is an age-dependent clinical milestone in multiple sclerosis, Multiple Sclerosis Journal 19 (2013) 188–198.

[81] D. M. Ha, J. Xu, J. S. Janowsky, Preliminary evidence that long-term estrogen use reduces white matter loss in aging, Neurobiology of aging 28 (2007) 1936–1940.

[82] S. M. Resnick, M. A. Espeland, S. A. Jaramillo, C. Hirsch, M. L. Stefanick, A. M. Murray, J. Ockene, C. Davatzikos, et al., Postmenopausal hormone therapy and regional brain volumes: the whims-mri study, Neurology 72 (2009) 135–142.

[83] K. Kantarci, N. Tosakulwong, T. G. Lesnick, S. M. Zuk, J. L. Gunter, C. E. Gleason, W. Wharton, N. M. Dowling, P. Vemuri, M. L. Senjem, et al., Effects of hormone therapy on brain structure: a randomized controlled trial, Neurology 87 (2016) 887–896.

[84] K. Yaffe, M. Haan, A. Byers, C. Tangen, L. Kuller, Estrogen use, apoe, and cognitive decline: Evidence of gene–environment interaction, Neurology 54 (2000) 1949–1954.

[85] J. Manly, C. Merchant, D. Jacobs, S. Small, K. Bell, M. Ferin, R. Mayeux, Endogenous estrogen levels and alzheimer's disease among postmenopausal women, Neurology 54 (2000) 833–837.

[86] C. Barth, A.-M. G. de Lange, Towards an understanding of women's brain aging: the immunology of pregnancy and menopause, Frontiers in Neuroendocrinology (2020) 100850.

[87] E. Baulieu, M. Schumacher, Neurosteroids, with special reference to the effect of progesterone on myelination in peripheral nerves, Multiple Sclerosis Journal 3 (1997) 105–112.

[88] C. Gregg, Pregnancy, prolactin and white matter regeneration, Journal of the neurological sciences 285 (2009) 22–27.

[89] D. Beck, A.-M. De Lange, I. I. Maximov, G. Richard, O. A. Andreassen, J. E. Nordvik, L. T. Westlye, White matter microstructure across the adult lifespan: A mixed longitudinal and cross-sectional study using advanced diffusion models and brain-age prediction, BioRxiv (2020).

[90] S. Tønnesen, T. Kaufmann, A.-M. de Lange, G. Richard, N. T. Doan, D. Alnaes, D. van der Meer, J. Rokicki, T. Moberget, I. I. Maximov, et al., Brain age prediction reveals aberrant brain white matter in schizophrenia and bipolar disorder: A multi-sample diffusion tensor imaging study, bioRxiv (2020) 607754.

[91] G. Richard, K. Kolskår, A.-M. Sanders, T. Kaufmann, A. Petersen, N. T. Doan, J. M. Sanchez, D. Alnaes, K. M. Ulrichsen, E. S. Dørum, et al., Assessing distinct patterns of cognitive aging using tissue-specific brain age prediction based on diffusion tensor imaging and brain morphometry, PeerJ 6 (2018) e5908.

[92] C. K. Tamnes, D. R. Roalf, A.-L. Goddings, C. Lebel, Diffusion mri of white matter microstructure development in childhood and adolescence: Methods, challenges and progress, Developmental cognitive neuroscience 33 (2018) 161–175.

[93] S. W. Davis, N. A. Dennis, N. G. Buchler, L. E. White, D. J. Madden, R. Cabeza, Assessing the effects of age on long white matter tracts using diffusion tensor tractography, Neuroimage 46 (2009) 530–541.

[94] A. B. Storsve, A. M. Fjell, A. Yendiki, K. B. Walhovd, Longitudinal changes in white matter tract integrity across the adult lifespan and its relation to cortical thinning, PloS one 11 (2016) e0156770.

[95] N. M. Armstrong, Y. An, L. Beason-Held, J. Doshi, G. Erus, L. Ferrucci, C. Davatzikos, S. M. Resnick, Sex differences in brain aging and predictors of neurodegeneration in cognitively healthy older adults, Neurobiology of aging 81 (2019) 146–156.

[96] D. K. Jones, M. Cercignani, Twenty-five pitfalls in the analysis of diffusion mri data, NMR in Biomedicine 23 (2010) 803–820.

[97] M. Habes, G. Erus, J. B. Toledo, T. Zhang, N. Bryan, L. J. Launer, Y. Rosseel, D. Janowitz, J. Doshi, S. Van der Auwera, et al., White matter hyperintensities and imaging patterns of brain ageing in the general population, Brain 139 (2016) 1164–1179.

[98] M. Anatürk, T. Kaufmann, J. H. Cole, S. Suri, L. Griffanti, E. Zsoldos, N. Filippini, A. Singh-Manoux, M. Kivimäki, L. T. Westlye, et al., Prediction of brain age and cognitive age: quantifying brain and cognitive maintenance in aging (2020).

[99] A. Fry, T. J. Littlejohns, C. Sudlow, N. Doherty, L. Adamska, T. Sprosen, R. Collins, N. E. Allen, Comparison of sociodemographic and health-related characteristics of uk biobank participants with those of the general population, American journal of epidemiology 186 (2017) 1026–1034.

[100] K. M. Keyes, D. Westreich, Uk biobank, big data, and the consequences of non-representativeness, The Lancet 393 (2019) 1297.

[101] C. Taylor, L. Pritschet, S. Yu, E. G. Jacobs, Applying a women's health lens to the study of the aging brain, Frontiers in Human Neuroscience 13 (2019) 224.

[102] H. Natri, A. R. Garcia, K. H. Buetow, B. C. Trumble, M. A. Wilson, The pregnancy pickle: Evolved immune compensation due to pregnancy underlies sex differences in human diseases, Trends in Genetics 35 (2019) 478–488.

[103] E. Nichols, C. E. Szoeke, S. E. Vollset, N. Abbasi, F. Abd-Allah, J. Abdela, M. T. E. Aichour, R. O. Akinyemi, F. Alahdab, S. W. Asgedom, et al., Global, regional, and national burden of alzheimer's disease and other dementias, 1990–2016: a systematic analysis for the global burden of disease study 2016, The Lancet Neurology 18 (2019) 88–106.